Neuron, Vol. 23, 715–724, August, 1999, Copyright ©1999 by Cell Press

Schwann Cell–Derived Desert Hedgehog Controls the Development of Peripheral Nerve Sheaths

Eric Parmantier,* Bruce Lynn,† Durward Lawson,‡ Mark Turmaine,* Soheila Sharghi Namini,* Lisa Chakrabarti,* Andrew P. McMahon,§ Kristjan R. Jessen,* and Rhona Mirsky*‖

*Department of Anatomy and Developmental Biology
†Department of Physiology
‡Department of Molecular Pathology
University College London
Gower Street
London WC1E 6BT
United Kingdom
§Department of Molecular and Cellular Biology
The Biolabs
Harvard University
Cambridge, Massachusetts 02138

Summary

We show that Schwann cell–derived Desert hedgehog (Dhh) signals the formation of the connective tissue sheath around peripheral nerves. mRNAs for *dhh* and its receptor *patched* (*ptc*) are expressed in Schwann cells and perineural mesenchyme, respectively. In $dhh^{-/-}$ mice, epineurial collagen is reduced, while the perineurium is thin and disorganized, has patchy basal lamina, and fails to express connexin 43. Perineurial tight junctions are abnormal and allow the passage of proteins and neutrophils. In nerve fibroblasts, Dhh upregulates *ptc* and *hedgehog-interacting protein* (*hip*). These experiments reveal a novel developmental signaling pathway between glia and mesenchymal connective tissue and demonstrate its molecular identity in peripheral nerve. They also show that Schwann cell–derived signals can act as important regulators of nerve development.

Introduction

Two fundamentally different ways have evolved for the mechanical protection of the mammalian nervous system. In the cases of the brain and the spinal cord, protection comes from sheltering inside the skull and the vertebrae, respectively. For peripheral nerves, however, the inflexibility and bulk that come with a bony encasing are not an option. Instead, the problem of protection has been solved by embedding the nerve fibers in a remarkably strong and flexible cable, or nerve sheath, made from collagen fibers and a cellular tube, the perineurium, that also acts as a barrier against unwanted molecules and cellular infiltration. In the present work, we have found that this protective structure is organized by the signaling protein Desert hedgehog (Dhh), originating from Schwann cells inside the nerve. Using genetically modified mice, we show that in the absence of this signal, the collagen fibers that give nerves their mechanical strength are dramatically reduced in number. Furthermore, the development of the perineurial tube is arrested at an early stage, resulting in a functionally impaired tube that leaves the nerve fibers unprotected against invading macromolecules or migrating cells. Significantly, we find that if inflammation is caused in the vicinity of nerves in which Dhh is missing, inflammatory cells have ready access to the nerve fibers, while in normal nerves, the perineurium provides a barrier that protects nerve fibers from inflammatory cells.

Dhh and its relatives have important signaling functions during early development (Tabin and McMahon, 1997; Ingham, 1998). The preliminary observation that mRNA for *dhh* was present in some early embryonic mouse nerves (Bitgood and McMahon, 1995) led us to investigate the role of Hedgehog signaling in peripheral nerve development. Dhh is a member of the Hedgehog family of signaling proteins, which, in the mouse, consists of three members: Sonic (Shh), Dhh, and Indian hedgehog (Ihh), all of which share a striking homology with the *Drosophila* segment polarity gene *hedgehog*, a key regulator of pattern formation in the embryonic and adult fly (Hammerschmidt et al., 1997). All of these genes encode secreted proteins. These proteins undergo a unique autoprocessing reaction, which leads to the generation of an active amino-terminal-derived ligand, containing a covalent attachment to cholesterol at its carboxyl terminus, that attaches the Hedgehog ligand to the cell surface (Tabin and McMahon, 1997). Shh is known to play crucial signaling roles in vertebrate development, including neural development, limb development, and the formation of sclerotome, vertebrae, and ribs (Hammerschmidt et al., 1997; Ingham, 1998). Relatively less is known about the roles of Dhh and Ihh, although Ihh is known to participate in chondrocyte differentiation (Vortkamp et al., 1996). *dhh* is expressed in testis, and a $dhh^{-/-}$ mouse failed to develop mature spermatozoa, indicating a requirement for *dhh* in spermatogenesis. It was suggested that this involved signaling by Dhh secreted by Sertoli cells (Bitgood and McMahon, 1995; Bitgood et al., 1996).

The signaling pathways used by Hedgehog proteins are complex, but the receptor for both Shh and Dhh is the 12 multiple-pass transmembrane tumor suppressor protein Patched (Ptc) (Goodrich et al., 1996; Stone et al., 1996). Ptc forms a complex with the serpentine transmembrane protein Smoothened (Smo) (Stone et al., 1996). Evidence from studies in *Drosophila* suggests that Ptc represses Smo. Binding of Hedgehog to Ptc releases this repression, resulting in activation of Smo and downstream signaling. Hedgehog binding to Ptc also upregulates expression of Ptc, which is thought to limit the spread of the ligand (Chen and Struhl, 1996). Other components of the Hedgehog signaling mechanism include protein kinase A, the Gli family of transcription factors, and Hedgehog-interacting protein (Hip) (see

‖To whom correspondence should be addressed (e-mail: r.mirsky@ucl.ac.uk).

Tabin and McMahon, 1997; Ingham, 1998; Chuang and McMahon, 1999).

We report here on the role of Dhh in the organogenesis of peripheral nerves. This process involves the recruitment of neurons, glia (Schwann cells), blood vessels, fibroblasts, and extracellular matrix to build a structure that will allow the ready and uninterrupted conduction of impulses along axons in an environment that is subject to ongoing movement and continuous mechanical stress. The generation of nerves begins with only two of these components, axons and Schwann cell precursors, which initially find their way through mesenchymal tissue, toward their targets, as compact structures essentially without intrinsic blood vessels or connective tissue. There are no careful studies of how or when vessels enter nerves, but in the rat hindlimb, nerves, blood vessels, and connective tissue are present by embryonic stage 17–18 (E17–E18) (generally corresponding to E15–E16 in the mouse) (Y. Hashimoto et al., unpublished data). At about this time, mesenchymal cells begin to be recruited to the nerves from their immediate environment and can be seen forming an irregular and incomplete lining around the larger diameter nerve branches. During the next 2–3 weeks, these cells complete a mesenchymal–epithelial transformation, generating a compact multilayered cellular tube, the perineurium (Kristensson and Olsson, 1971; Thomas and Olsson, 1984; Bunge et al., 1989; Olsson, 1990; Schiavinato et al., 1991). The perineurial cells are flattened and, in each layer, align together in a pavement-like manner comparable to that seen in the endothelial lining of blood vessels; they are then sealed by tight junctions and form an effective diffusion barrier. They are also lined by a prominent basal lamina. The nerve is reinforced by heavy deposits of collagen both inside the perineurium, among the nerve fibers in the endoneurium, and in a distinct layer immediately outside the perineurial tube, the epineurium. Together, the endo-, peri-, and epineurium constitute the protective nerve sheath.

The experiments described here reveal the existence of a novel developmental signaling pathway between glia and mesenchymal tissue and demonstrate its molecular identity in peripheral nerve. The finding that Schwann cell–derived Dhh controls the formation of nerve sheaths also shows that Schwann cells can act as important regulators of nerve development, a notion that is now supported by a rapidly increasing number of observations (Jessen and Mirsky, 1999).

Results

dhh Is Expressed by Schwann Cells throughout Development

To investigate the pattern of *dhh* expression during peripheral nerve development, in situ hybridization was carried out on polyester wax sections of E13 and E15 embryos and on teased nerves from postnatal animals. At E13, when the developing nerves are populated by Schwann cell precursors (Jessen et al., 1994; Dong et al., 1995, 1999), *dhh* transcripts were expressed by Schwann cell precursors both in the dorsal and ventral roots and in the emerging spinal nerves. At E15, a stage when the sciatic nerve and brachial plexus are mostly populated by Schwann cells (Dong et al., 1999), a signal was also detectable in growing nerves out in the hindlimb (data not shown). Using teased nerve preparations, we found that *dhh* mRNA is expressed in Schwann cells of newborn, postnatal day 5 (P5) and P10 nerves (Figures 1A–1C), while in adult nerves, very few cells expressed *dhh* at levels that were detectable in the present experiments. When in situ hybridization was combined with immunocytochemistry for GAP-43 to specifically label nonmyelinating Schwann cells (Curtis et al., 1992) on teased nerve preparations from P10 rats, it was apparent that the postnatal expression of *dhh* was essentially restricted to myelinating Schwann cells (Figures 1B and 1C). This was confirmed by double labeling for *dhh* and myelin basic protein (data not shown).

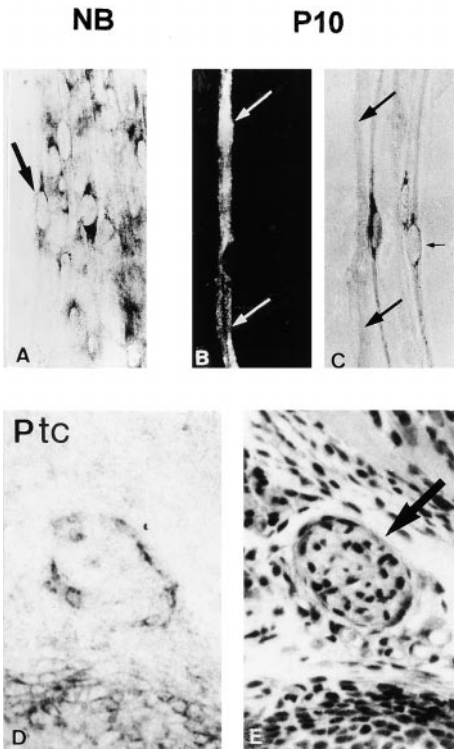

Figure 1. *dhh* and *ptc*, Visualized by In Situ Hybridization Using a DIG-Labeled Riboprobe, Are Associated with Peripheral Nerves

(A) In teased preparations of newborn nerve, *dhh* is detectable in the perinuclear areas of most/all Schwann cells (arrow).

(B and C) In teased nerve preparations of P10 nerves, a combination of in situ hybridization and immunocytochemistry, using antibodies to GAP-43 (B), a marker of nonmyelinating Schwann cells, revealed that *dhh* expression is restricted to myelinating Schwann cells. Tilted arrows point to a GAP-43-positive fiber and horizontal arrow to the nucleus of a *dhh*-positive cell (C).

(D) In contrast to *dhh*, *ptc* is seen in a restricted population of mesenchymal cells located at the outer margins of a nerve at E15. Low levels of signal are associated with occasional cells within the nerve bundle. *ptc* signal is also found in cells in the region of developing cartilage (bottom), where Ihh signals play a role.

(E) Toluidine blue–stained section shows the nerve (arrow). Developing cartilage is present in the lowest part of the picture.

The *dhh* Receptor *ptc* Is Expressed in Developing Peripheral Nerve

The above experiments raised the possibility that Schwann cell–derived Dhh had some role in the regulation of nerve development. To localize potential target cells of

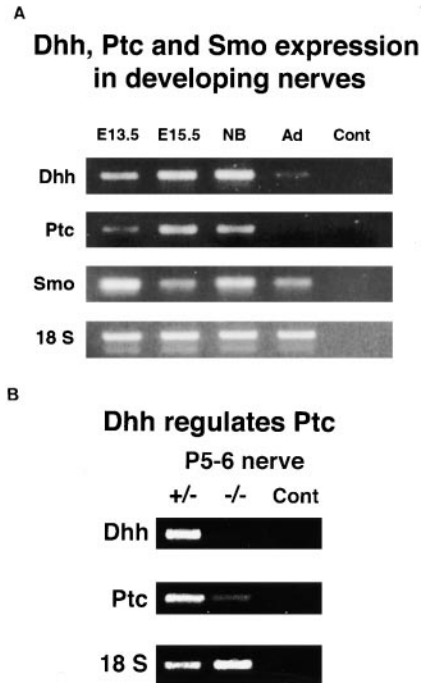

Figure 2. *dhh*, *ptc*, and *smo* Are Detectable by Semiquantitative RT-PCR in Sciatic Nerves from Normal Mice of Different Developmental Ages, and *ptc* Levels Are Regulated by *dhh*

(A) Comparison of mRNA levels for *dhh*, *ptc*, and *smo* in normal nerves taken at different developmental stages. Note that levels of *dhh* and *ptc* remain relatively steady from E13 until birth (NB) but that much lower levels are detectable in adult (Ad) nerves, while *smo* levels remain relatively unchanged with developmental age. Although *ptc* was not detectable in adult nerve under the conditions used here, it was seen when higher amounts of mRNA were used in the RT-PCR reaction (data not shown). Water controls (Cont) were negative.

(B) In $dhh^{-/-}$ nerves from P5–P6 rats, *dhh* is undetectable, while *ptc* levels are much lower than in $dhh^{+/-}$ nerves.

Dhh signals, a digoxygenin- (DIG-) labeled *ptc* probe was used in in situ hybridization experiments. At E15, a clear ring of *ptc* expression was seen in a restricted population of cells at the outer margins of nerve bundles (Figures 1D and 1E). Based on their location and morphology, we can assume that these cells are epineurial/perineurial precursors. A weaker *ptc* signal was also detected in the perineurium of newborn nerves (data not shown). A low level of signal could also be seen in a few discrete areas within the nerve. Taken together, these results suggest that Dhh secreted by Schwann cells is involved in the differentiation of the connective tissues surrounding the nerve.

mRNA Corresponding to *dhh*, *ptc*, and *smo* Is Present in Peripheral Nerves by RT-PCR

Semiquantitative RT-PCR was carried out on mRNA extracted from nerves from E13, E15, newborn, and adult mice. The *dhh* signal was strongest in E15 and newborn nerves, declining in adult nerves, in accordance with the in situ data. The expression of *ptc* was broadly similar, while mRNA for the Ptc-associated transmembrane protein Smo could be detected at all ages tested (Figure 2A).

To determine whether the level of *ptc* mRNA in peripheral nerve was affected by levels of Dhh present in Schwann cells, *ptc* mRNA was estimated by semiquantitative RT-PCR in P5–P6 $dhh^{+/-}$ and $dhh^{-/-}$ mice, a stage when the perineurium is beginning to mature (Kristensson and Olsson, 1971). *dhh* was undetectable in $dhh^{-/-}$ nerves, as expected, while levels of *ptc* were much reduced in comparison with $dhh^{+/-}$ nerves (Figure 2B). This suggests that Dhh controls *ptc* expression levels in the perineurium, as seen for hedgehog proteins and Ptc in other systems (Tabin and McMahon, 1997).

In $dhh^{-/-}$ Mice, the Differentiation of the Epi-, Peri-, and Endoneurium Is Abnormal

These results suggested that Dhh might be involved in signaling from Schwann cells to mesenchymal cells, and, therefore, in the organization of the connective tissue around nerve fibers. Consequently, we compared the morphology of the sciatic nerve in adult $dhh^{-/-}$ and normal mice by electron microscopy, paying particular attention to the organization of the epi-, peri-, and endoneurial connective tissues (Figure 3A). On dissection, the $dhh^{-/-}$ nerves appeared flattened rather than round. As described previously, in the normal mouse, the epineurium is mainly formed of collagen fibrils and of scattered fibroblasts lacking a basal lamina. The perineurium is formed from a succession of compacted layers of flattened cells of epithelial-like morphology (six to eight) concentrically arranged around the nerve. The cells appear taut and flattened, with a basal lamina on each side. Within each layer, the cells are linked together by tight junctions and gap junctions (Thomas and Olsson, 1984). The barrier to molecular and cellular infiltration into the nerve is established by the perineurium (Olsson, 1990). The layered arrangement makes it easy in normal nerves to recognize the boundary between the perineurium and the epineurium on one side and the endoneurium on the other (Figure 3B). In comparison, in the $dhh^{-/-}$ nerve, clear differences could be seen in the organization of the nerve sheath. The epi- and perineurium were much less compacted, and there was much less collagen in the epineurium; in some places it appeared to be almost absent. The number of layers forming the perineurium varied around the nerve (two to four) but was always less than that in control nerves (Figures 3D and 3E). The concentric layers were not in close contact with each other and had a loose and wavy disposition. Furthermore, the cells in the mutant perineurium had a discontinuous basal lamina, making it difficult to pinpoint the boundary between epi- and perineurium. Perineurial cells in both normal and null mice were characterized by the presence of numerous caveolae along their surface, and junctional contacts could be seen. The nerve fibers within $dhh^{+/-}$ nerves appeared normal at both the light and electron microscope levels.

The ultrastructural analysis also revealed that in the $dhh^{-/-}$ nerve, cells with the characteristics of mutant perineurial cells had invaded the endoneurial space. In the control nerves, endoneurial fibroblasts had triangular or rectangular perikarya, with cytoplasm characterized by a prominent, rough endoplasmic reticulum and pinocytotic vesicles. They sent out processes that elongated between myelinating and nonmyelinating fibers and in transverse sections were seen relatively rarely. As in the epineurium, normal endoneurial fibroblasts lacked a basal lamina. In contrast, in the $dhh^{-/-}$ nerve, few

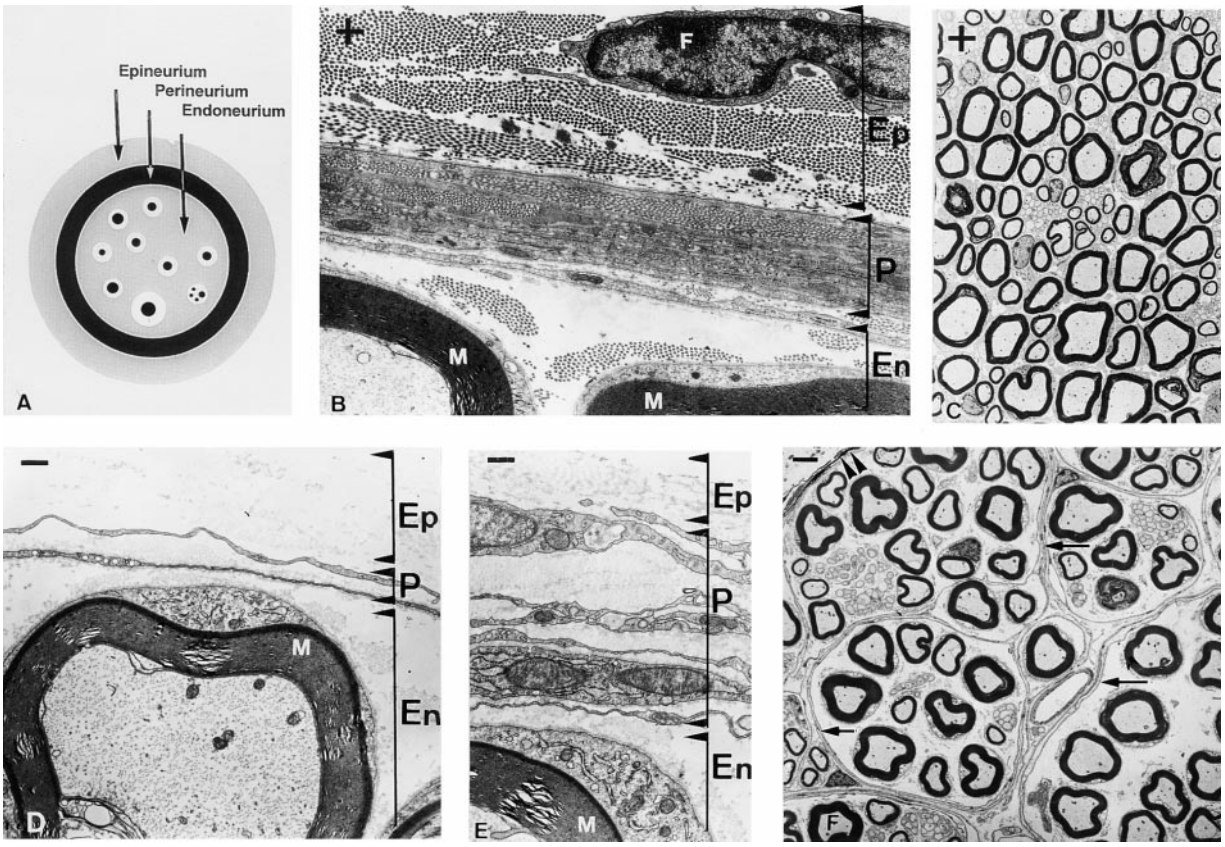

Figure 3. By Electron Microscopy, the Epi-, Peri-, and Endoneurium of *dhh*$^{-/-}$ Nerves Are Abnormal

(A) Diagram of the organization of epi-, peri-, and endoneurial connective tissue shown in a transverse section from normal nerve.

(B) In normal (plus) sciatic nerve, the epineurium (Ep) consists mainly of collagen fibrils and of scattered fibroblasts (F) lacking a basal lamina. The perineurium (P) consists of six to eight layers of compacted concentric layers of flattened cells with a continuous basal lamina on each side. Parts of two myelinated axons in the intrafascicular space, surrounded by endoneurial (En) collagen fibrils, can be seen in the lower part of the micrograph. Abbreviation: M, myelin sheaths.

(C) Low-power view of a normal (plus) nerve, showing myelinated axons of various diameters as well as unmyelinated fibers. Note the absence of compartments.

(D and E) In *dhh*$^{-/-}$ nerves (minus), the epineurium (Ep) is extremely thin, with many fewer collagen fibrils. The number of perineurial (P) layers varies around the nerve (compare [C] and [D]) but is always less than in normal nerve taken at the same level. In addition, the cytoplasm is much less compacted, the basal lamina is patchy rather than continuous, and the cells have an undulating, disorganized appearance. Like normal perineurial cells, the *dhh*$^{-/-}$ perineurial cells have prominent caveolae at intervals along the plasma membrane. Abbreviation: M: myelin sheaths.

(F) Low-power view of the interior of a *dhh*$^{-/-}$ nerve (minus). Note the presence of several prominent minifascicles, each consisting of several layers of cells with perineurial characteristics (arrows), i.e., patchy basal lamina, and as shown in Figure 6, prominent caveolae and junctional complexes enclosing variable numbers of myelinated and unmyelinated fibers. In one of the minifascicles, which contains only myelinated fibers (bottom right), the collagen fibrils are extremely sparse. This is typical of areas where no unmyelinated fibers are present. Double arrowheads, the perineurium of the surface of the nerve.

typical fibroblasts could be seen, and the interior of the nerve was divided into compartments, often called minifascicles, by flattened, perineurial-like cells. The walls of these compartments consisted of one to six cell layers (Figure 3F). These mutant perineurial-like cells invading the endoneurial space had a discontinuous basal lamina and established junctions where their processes came in contact. They were indistinguishable from the mutant perineurial cells at the edge of the nerve (Figures 3D–3F and Figure 4).

The ultrastructures of both myelinated and unmyelinated fibers appeared normal, and the ratio of myelinated to unmyelinated axons was the same in normal and mutant nerves despite the aberrant organization into minifascicles. Some minifascicles consisted solely of myelinated fibers. Although a comprehensive quantitative analysis was not made, there appeared to be fewer collagen fibrils in the endoneurial space of these fascicles than in the normal nerve or in minifascicles containing a mixture of myelinated and unmyelinated fibers.

To determine whether the differences between normal and mutant animals were present from the onset of connective tissue sheath formation, we examined nerves from E15 and E16 mice by electron microscopy. Consistent differences in the developing perineurium/epineurium were not seen between normal and *dhh*$^{-/-}$ nerves, suggesting that Dhh signaling is involved in later stages of perineurial sheath maturation. In most cases, a developing perineurial sheath consisting of several fairly loosely compacted layers could be seen, although

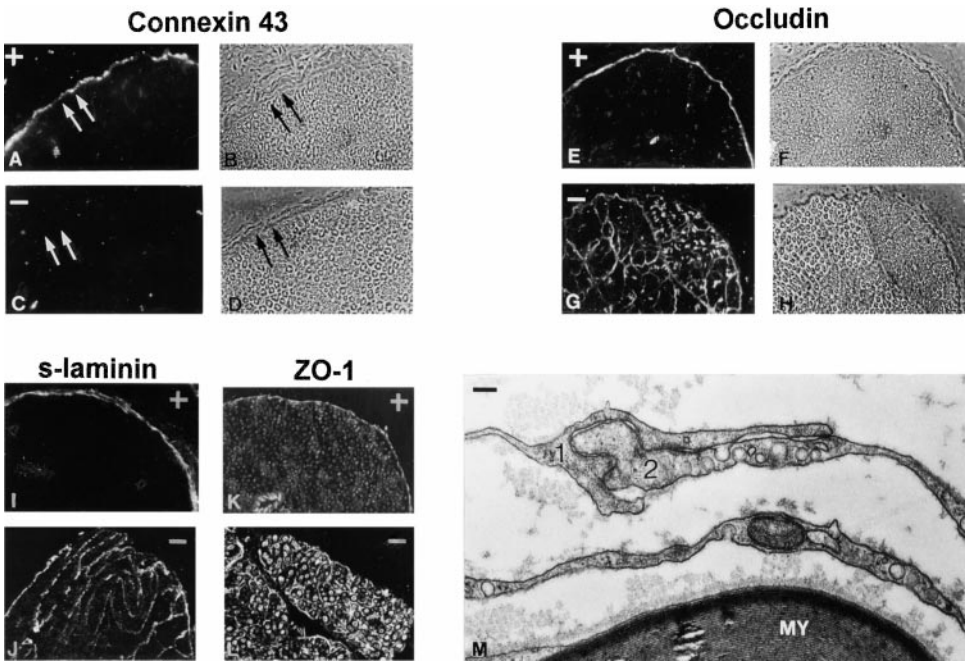

Figure 4. The Cells Forming Minifascicles in Mutant Nerves Have the Antigenic Phenotype of Immature Perineurial Cells and Do Not Express Connexin 43

(A–D) Comparison of connexin 43 immunolabeling in transverse sections from normal and *dhh*$^{-/-}$ nerves. Normal nerves are indicated by (plus); *dhh*$^{-/-}$ nerves by (minus).

(A) Connexin 43 is expressed in the perineurial cells of normal nerve (double arrows), seen by phase contrast in (B).

(C) In contrast, in *dhh*$^{-/-}$ nerve, connexin 43 is not expressed by perineurial cells at the edge of the nerve (location indicated by double arrows) or in the cells of the minifascicles that occupy the interior of these nerves.

(E–H) Comparison of occludin immunolabeling in transverse sections from normal and *dhh*$^{-/-}$ nerves.

(E) Occludin is expressed by perineurial cells at the edge of the normal nerve, seen by phase contrast in (F).

(G) in *dhh*$^{-/-}$ nerves, occludin is also expressed by perineurial cells at the edge of the nerve, seen by phase contrast in (H), and in cells of the minifascicles throughout the nerve. Note that occludin labeling emphasizes the differences in perineurial architecture and compartmentation between the two nerves.

(I and J) Immunolabeling for laminin β2, in transverse/oblique sections from a normal and a *dhh*$^{-/-}$ nerve.

(I) In normal animals, laminin β2 is restricted to the perineurium at the edge of the nerve.

(J) Like occludin, in *dhh*$^{-/-}$ nerve, laminin β2 is present in the primitive perineurium at the edge of the nerve and in the cells of the minifascicles.

(K and L) Immunolabeling for ZO-1 in transverse section from a normal and a *dhh*$^{-/-}$ nerve. Again, in normal nerve, labeling is seen at the edge of the nerve, while in *dhh*$^{-/-}$, nerve labeling is seen in perineurial cells at the edge of the nerve and in the cells of the minifascicles. It is also seen at the junction between the axonal membrane and the adaxonal Schwann cell membrane in both normal and *dhh*$^{-/-}$ nerves.

(M) Electron micrograph of cells of a minifascicle in a *dhh*$^{-/-}$ nerve. Note the intercellular junctions between cells 1 and 2, the presence of caveolae typical of normal perineurial cells, and the presence of a patchy basal lamina that contrasts with the apparently normal basal lamina on the myelinating Schwann cell (MY).

occasionally in the mutant nerves, the sheath appeared to be less well developed (data not shown).

Connexin 43 Is Not Expressed by Perineurial Cells in *dhh*$^{-/-}$ Mice, although Occludin, Laminin β2, and ZO-1 Are Present

To investigate whether the molecular phenotype of the mutant perineurial cells is different from that of normal perineurial cells, we used antibodies to several known molecular markers of perineurial cells. Antibodies to the gap junction protein connexin 43, present in perineurial cells (Chandross et al., 1996), revealed a clear difference between *dhh*$^{+/+}$ *and dhh*$^{-/-}$ animals. In normal nerves, a continuous ring of labeling was seen in the position of the perineurium, while in mutant nerves, there was no labeling either around or within the nerve (Figures 4A–4D). Thus, the mutant cells with perineurial morphology at the edge of the nerve and those forming the minifascicles within it lack this gap junction protein. Antibodies to the major tight junction protein occludin (Furuse et al., 1993) highlighted the differences in connective tissue organization between normal and *dhh*$^{-/-}$ nerves. In normal nerves, there was a ring of labeling associated with the perineurium as well as some labeling within the endoneurium, associated with nerve fibers. There was no labeling of fibroblastic cells in the endoneurium. In *dhh*$^{-/-}$ nerves, however, occludin labeling was seen not only around the nerve but also within it, in the position of the minifascicles, revealing their organization clearly (Figures 4E–4H). Another perineurial marker, laminin β2 (Sanes et al., 1990), showed a similar distribution since it was detectable on normal perineurial cells around the nerve and on mutant perineurial cells around the nerve and in the minifascicles (Figures 4I and 4J). The junction-associated protein ZO-1 (Stevenson et al., 1986) and the glucose transporter protein Glut-1 (data not shown) were located in a similar pattern. In addition to expression in perineurial cells, ZO-1 was also present at the

junction between the axons and the adaxonal Schwann cell surface in myelinated axons (Figures 4K and 4L). This was seen both in normal and mutant nerves. The junctions formed between the perineurial cells that constitute the minifascicles are shown at the ultrastructural level in Figure 4M.

The Nerve–Tissue Barrier Is Defective in *dhh*$^{-/-}$ Mice

Since minifascicles are normally formed around regrowing axon–Schwann cell units during nerve regeneration, when the normal nerve–tissue barrier is breached, we hypothesized that the integrity of this barrier in mutant nerves might be compromised (Thomas and Jones, 1965; Ahmed and Weller, 1979; Hall, 1989). To test this, we injected Evans blue albumin (EBA), a large molecular weight tracer previously used to measure the integrity of the barrier, in the vicinity of the sciatic nerve (Thomas and Olsson, 1984). After 1 hr, the nerves were excised and processed for fluorescence microscopy. When normal and mutant nerves were compared, there was virtually no penetration of the dye complex into the endoneurium of the normal nerve, whereas the mutant nerve was labeled throughout, clearly establishing that the nerve–tissue barrier was defective (Figures 5A and 5B). In normal nerves, it has also been shown that the perineurial barrier protects the nerve fibers from invasion by bacteria since nerves running through inflamed tissues are devoid of inflammatory cells (Thomas and Olsson, 1984). To induce an inflammatory response and test the integrity of the nerve–tissue barrier to inflammatory cells, we injected suspensions of heat-killed *Escherichia coli* in the vicinity of the nerve. At 24 and 48 hr and 15 days, the animals were killed and the nerves processed for light or electron microscopy. Using a granulocyte-specific antibody, Ly6-G (Lagasse and Weissman, 1996), to reveal granulocytes, no granulocytes could be seen within the normal nerves at 24 hr or 48 hr, while granulocytes were clearly visible in *dhh*$^{-/-}$ nerves (Figures 5C and 5D). This result was confirmed by hematoxylin and eosin staining, when neutrophils could be seen outside but not within normal nerves, but both outside and within mutant nerves (data not shown). In the electron microscope, again neutrophils could be seen within the mutant nerves but not in normal nerves at 24 or 48 hr postinjection (Figure 5E).

Freeze-Fracture Electron Microscopy Reveals Abnormal Tight Junctional Arrays in *dhh*$^{-/-}$ Mice

To investigate whether the tight junction network was compromised structurally, nerves from adult normal and *dhh*$^{-/-}$ mice were fixed and observed by freeze-fracture electron microscopy. The perineurium of normal animals showed large junctions consisting of complex multistranded, anastomosing networks as previously reported (Figure 6B) (Schiavinato et al., 1991; Beamish et al., 1992). Junctions of this kind were not found in the perineurium of *dhh*$^{-/-}$ mice. Rather, we saw much simpler assemblies of junctional strands, which were less well ordered, with fewer anastomosing strands. In addition, individual strands showed multiple interruptions when compared with strands in tight junctions of normal perineurium (Figure 6A).

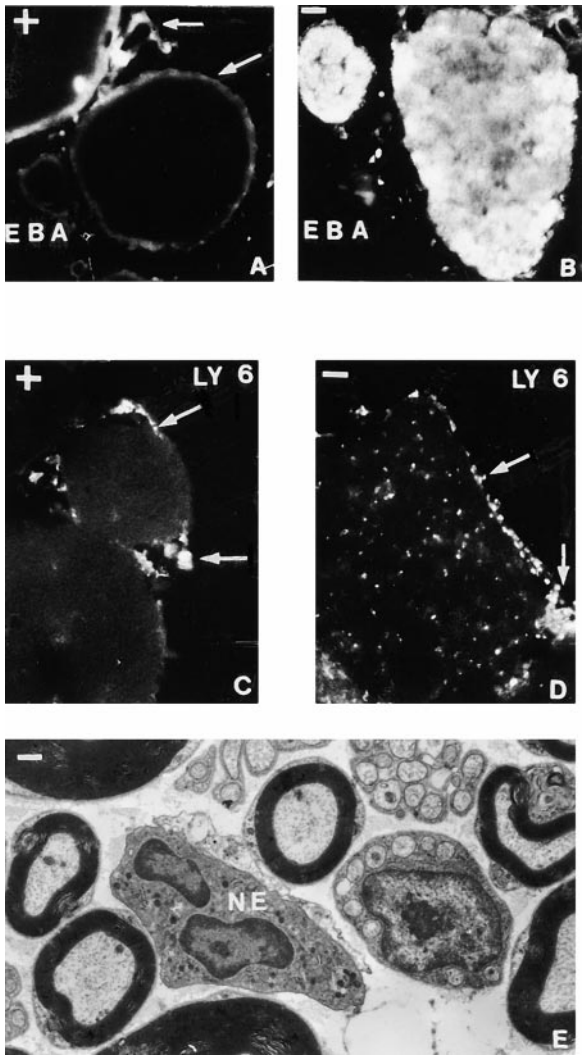

Figure 5. Perineurial Permeability Is Abnormal in *dhh*$^{-/-}$ Mice

Normal nerves are indicated by (plus); *dhh*$^{-/-}$ nerves by (minus).

(A) Following injection of EBA in the vicinity of normal nerves, EBA can be seen sticking to the extraneural connective tissue (horizontal arrow) and the epineurium/perineurium (tilted arrow). Note that EBA has not penetrated the interior of any of the three nerve bundles shown.

(B) In contrast, when EBA is injected near *dhh*$^{-/-}$ nerves, the protein completely permeates the interior of both large and small nerve bundles as shown.

(C and D) When an immune response is elicited by injection of bacteria in the vicinity of nerves, neutrophils, visualized here by Ly6-G antibody, are barred from entering normal nerves (C) but migrate throughout the interior of *dhh*$^{-/-}$ nerves (D). In both normal and *dhh*$^{-/-}$ nerves, neutrophils accumulate outside the nerve bundles (horizontal arrows) and are found in the epineurium (tilted arrows).

(E) Electron micrograph showing a neutrophil (NE) within a *dhh*$^{-/-}$ nerve after bacterial challenge.

Dhh Induces *ptc* and *hip* Upregulation in Cultured Nerve Fibroblasts

The localization of *ptc* in the mesenchyme immediately surrounding developing nerves (see above) indicated strongly that these cells are a target of Dhh signaling. To confirm that Dhh could act directly on fibroblastic cells, immunopurified fibroblasts were exposed to Dhh

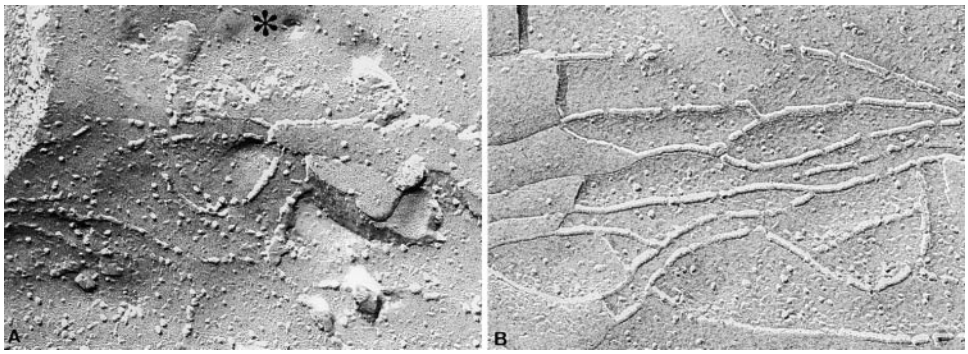

Figure 6. Freeze-Fracture Electron Micrograph Showing the Structure of Tight Junctions between Perineurial Cells in $dhh^{-/-}$ and Normal Nerves

Note the poorly developed and discontinuous junctional arrays in the $dhh^{-/-}$ perineurium, compared with the orderly and relatively continuous network in the normal perineurium. A perineurial caveolus is asterisked. Magnification, ×130,000.

protein for time periods of up to 24 hr. Induction of *ptc* and the associated gene *hip* was monitored by semiquantitative RT-PCR. Clear induction of *ptc* and *hip* was seen in response to Dhh (Figure 7). mRNA for the Ptc-associated molecule *smo* was also present, confirming the existence of another component of Dhh signaling pathways in these cells. Smo levels remained relatively unchanged over a period of 24 hr (Figure 7). *Gli3*, another component of the Hedgehog signaling pathway, was also detectable (data not shown).

Nerve Conduction

As reported previously, the movements of $dhh^{-/-}$ and $dhh^{+/+}$ mice appear indistinguishable when they are running freely (Bitgood and McMahon, 1995). It was therefore unlikely that gross differences in myelination or nerve conduction velocity were present. We nevertheless examined the nerve conduction velocity of different fiber classes in more detail in view of the abnormalities in permeability and connective tissue organization. The data are summarized in Table 1. When the motor conduction velocity, the saphenous A fiber conduction velocity, and the saphenous C fiber conduction velocity are compared between groups of $dhh^{+/+}$ *and* $dhh^{-/-}$ mice, in each case, the nerve fibers measured in $dhh^{-/-}$ animals showed on average a lowered velocity. Nevertheless, the differences were not statistically significant in any of the three cases, and considerably larger groups of animals would be required to resolve this issue. Threshold and compound potential amplitude did not show consistent change between the two groups of animals.

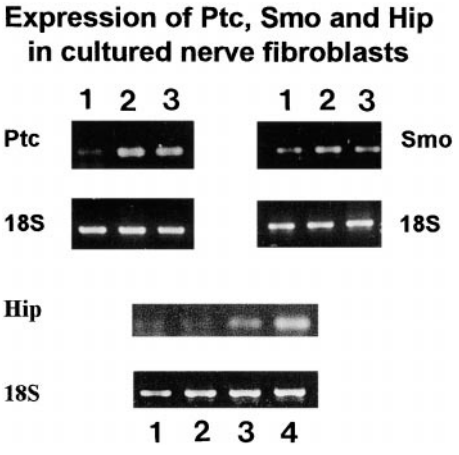

Figure 7. *ptc*, *smo*, and *hip* Are Detectable by Semiquantitative RT-PCR in Nerve-Derived Fibroblasts, and *ptc* and *hip* Levels Are Regulated by *dhh*

(Left) Comparison of mRNA levels for *ptc* before (1) and after treatment for (2) 3 hr and (3) 24 hr with Dhh. Note that treatment with Dhh upregulates the levels of *ptc*.

(Right) *smo* levels before (1) and after treatment with Dhh for (2) 2 hr and (3) 3 hr. Smo levels appear relatively unchanged.

(Bottom) *hip* levels before (1) and after treatment with Dhh for (2) 1 hr, (3) 2 hr, and (4) 24 hr. Note that treatment with Dhh upregulates the levels of *hip*; 18S levels are shown below.

Discussion

The work presented here shows that the Schwann cell–derived signal Dhh controls the development of the peripheral nerve sheath and the transition of mesenchymal cells to form the epithelium-like structure of the perineurial tube. As a consequence of lack of Dhh, the morphology of the adult nerve is grossly abnormal, and the perineurial cells fail to express the gap junction protein connexin 43. The perineurial barrier is leaky and allows the entry of both proteins and unwanted cells. By freeze-fracture electron microscopy, we find that this is due to a marked disorganization of the tight junctional arrays that normally form between perineurial cells.

All three components of the sheath are strongly affected by the absence of Dhh in vivo. In the epineurium, the chief consequence is a reduction in collagen, while in the cases of the perineurium and the endoneurium, the picture is more complex. Our interpretation is that the formation of the perineurium occurs in at least two major stages (Figure 8). The first includes the initial recruitment of mesenchymal cells and their alignment to generate a thin, loose, and permeable sheath. This stage is comparable in the embryonic nerves of normal and $dhh^{-/-}$ mice, and we conclude on the basis of this, and arguments outlined below, that Dhh is not essential for these early events. The second stage involves the embellishment of the primitive sheath to form an ordered

Table 1. Nerve Conduction Velocities in $Dhh^{+/+}$ and $Dhh^{-/-}$ Peripheral Nerves

Type		SaphA-cvm/s	SaphC-cvm/s	SciMot-cvm/s
$Dhh^{+/+}$	average	29.90	0.78	38.40
	SEM	2.50	0.06	3.00
	n =	2	3	2
$Dhh^{-/-}$	average	28.29	0.67	33.05
	SEM	2.36	0.02	4.45
	n=	4	4	2
	probability (t test)	0.673	0.199	0.436
$Dhh^{-/-}/Dhh^{+/+}$ %	% change	−5.4%	−13.6%	−13.9%

Comparison of average nerve conduction velocities (cv) of the A and C fibers in the Saphenous nerve and of sciatic nerve motor fibers in $Dhh^{+/+}$ and $Dhh^{-/-}$ mice. Conduction velocities were measured as described in the Experimental Procedures. The number (n) of nerves used in each type of experiment is indicated. The t test results show that the percent decrease in nerve conduction velocity, seen in all three types of fibers, is not statistically significant.

multilayered structure, the elaboration of a mature basal lamina, expression of connexin 43, and the emergence of a functionally competent perineurium capable of excluding proteins and inflammatory cells. This developmental step does not occur in $dhh^{-/-}$ nerves. They remain surrounded by a perineurium similar to that seen in normal developing nerves. In this sense, the phenotype of the perineurial sheath in $dhh^{-/-}$ mice represents a developmental arrest, and we conclude that the second step of normal perineurial development depends on Dhh signaling from Schwann cells. The presence of *ptc* in mesenchymal cells around developing nerves, and the fact that Dhh upregulates *ptc* and also *hip* in nerve fibroblasts in culture, indicate that mesenchymal cells are direct targets of Dhh signaling during nerve development.

A striking feature of the mutant nerves is the extensive formation of multiple small compartments, minifascicles, inside the nerve. In normal animals, similar minifascicles form under conditions in which the perineurial barrier is damaged and the endoneurial environment is exposed to the surrounding tissues, e.g., following nerve transection or other breach of the perineurium (Thomas and Jones, 1965; Thomas and Bhagat, 1978; Ahmed and Weller, 1979; Bradley et al., 1998). Therefore, the formation of minifascicles in $dhh^{-/-}$ nerves is probably triggered by the leakiness of the perineurium; it would then be only an indirect consequence of the absence of Dhh signaling.

The minifascicles in $dhh^{-/-}$ nerves form loose tubes of cells that are continuous with the innermost layer of the primitive perineurium surrounding these nerves. Like the mutant perineurium, they express laminin β2, occludin, and ZO-1 but do not form effective diffusion barriers. Therefore, these structures inside the $dhh^{-/-}$ nerves are analogous to the primitive perineurium surrounding these nerves. It follows, as argued above, that they are comparable to immature perineurium around normal developing nerves. Thus, the presence of abundant minifascicles in $dhh^{-/-}$ nerves shows that a tissue similar to the normal immature perineurium forms readily in the absence of Dhh. This provides an additional reason to believe that *dhh* is not involved in the first step of normal perineurial development.

Our experiments with albumin injections showed that the $dhh^{-/-}$ perineurium cannot carry out its barrier function, generally considered to be one of the main functions of this tissue. This is clearly due to a functional defect in the tight junctions that normally form between perineurial cells. Although we find that junctional morphology is grossly abnormal in the mutant, this defect is not due to the absence of occludin or the associated protein ZO-1 since we found these molecules in the abnormal perineurium of $dhh^{-/-}$ nerves (Furuse et al., 1993, 1998a, 1998b; McCarthy et al., 1996; Wong and Gumbiner, 1997; Saitou et al., 1998). The lack of expression of connexin 43 in the perineurial cells of the mutant may be significant in view of the observation that the appearance of connexin 43 is associated with the transformation of embryonic corneal fibroblasts to stratified epithelium induced by transfection of E-cadherin (Vanderburg and Hay, 1996). Connexin 43 could therefore be required for proper interaction between cells in the inner perineurial layers, resulting in coordinate tight junction formation and the establishment of a tight nerve–tissue barrier (Elias and Friend, 1976; Schiavinato et al., 1991; Beamish et al., 1992; Kojima et al., 1996; Fujimoto et al., 1997; Simon and Goodenough, 1998). Another molecule that may be critical for perineurial formation is neurofibromin since normal perineurium

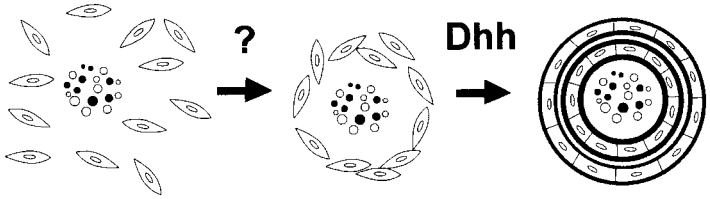

Figure 8. A Simplified Representation of the Development of the Perineurium as a Two-Step Process

Unknown signals (question mark) recruit connective tissue cells to form a loose permeable tube around embryonic nerves. Dhh from Schwann cells, probably acting together with other factors, is needed to transform this structure into an ordered, multilayered, mature perineurium that acts as a barrier against unwanted proteins and cells and thus to complete the mesenchymal–epithelial transition.

does not form in cocultures of fibroblasts from neurofibromin-deficient mice with normal Schwann cells and neurons (Rosenbaum et al., 1995). The target genes that Dhh activates in this system are likely to relate to epithelial differentiation and remain to be determined. Promotion of cell division is not likely to be an important function since we were unable to detect a significant effect of Dhh on DNA synthesis in nerve embryo–derived fibroblasts in vitro (data not shown).

The ready access of inflammatory cells to the nerves of *dhh*$^{-/-}$ animals reveals a fault in another main perineurial function, namely that of protecting nerves from bystander damage during local inflammatory episodes in the nerve environment. Inflammatory cells secrete a large number of bioactive factors that are potentially harmful to normal tissues (Gold et al., 1999). In the nervous system, the invasion of inflammatory cells has been associated both with acute effects due to secretion of molecules that already affect the function of neuronal proteins, including ion channels, and with long-term effects involving inflammatory tissue damage (Olsson, 1990). One of the clinical issues that arises from this work relates to a collection of poorly recognized pathology in humans which involves chronic and diffuse limb pain that is resistant to routine pain-killing drugs (Greening and Lynn, 1998). It is thought that these syndromes are caused by relatively subtle mechanical nerve injury and/or inflammation near or in the nerve sheath. Since Dhh signaling is involved in building the barriers that protect nerves against mechanical assault and inflammation-related damage, it will be of interest to examine whether failure of Dhh signaling contributes to these conditions. The extensive minifascicle formation in *dhh*$^{-/-}$ nerves is also reminiscent of focal hypertrophic neurofibrosis, a condition of unknown etiology, involving extensive endoneurial compartmentation (Thomas et al., 1990).

This study combines with other recent work to highlight a role for Schwann cells as important regulators of nerve development. Evidence suggests that in addition to their role in forming the nerve connective tissue sheaths, these cells provide essential survival factors for developing sensory and motor neurons, autocrine factors for their own postnatal survival in the absence of axons, and signals that regulate the formation of the Node of Ranvier and other aspects of axonal architecture (Jessen and Mirsky, 1999).

The formation of the perineurium shows many of the cardinal features of a mesenchymal–epithelium transformation, a process that occurs widely in embryogenesis but is poorly understood at the molecular level. In a broader context, the present results raise the possibility that Dhh may be more generally involved in directing such processes in other tissues or organs during development.

Experimental Procedures

Materials

Rabbit polyclonal antibodies to occludin and ZO-1 were from Zymed Labs (San Francisco, CA), rabbit polyclonal anti–connexin 43 antibody was a gift of Dr. R. Dermietzel (Bochum, Germany), rabbit polyclonal antibody to GAP-43 was from Dr. R. Curtis, and goat anti-rabbit immunoglobulin conjugated to fluorescein was from Cappel-Organon Technika (West Chester, PA). Alkaline phosphatase–conjugated sheep anti-digoxigenin antibody, 5-bromo-4-chloro-3-indolyl phosphate, and nitroblue tetrazolium salt were from Boehringer Mannheim (Lewes, UK). Rat monoclonal antibodies to Ly6-G (Gr-1) were from Pharmingen (San Diego, CA). Antibody to laminin β2 was a gift from Dr. J. Sanes (Porter and Sanes, 1995). Sources of other reagents used in immunocytochemistry, RT-PCR, and electron microscopy have been detailed in previous papers (Jessen et al., 1994; Dong et al., 1995; Blanchard et al., 1996).

Animals

The developmental analysis of *dhh*, *ptc*, and *smo* was carried out on Institute for Cancer Research mice. The *dhh* null mutant was obtained by homologous recombination as described previously (Bitgood et al., 1996). Animals were genotyped by PCR on genomic DNA with a set of three primers. Primers were designed as follows: gDhh1, 5′CCAGGAAGACGAGCACTGGCGTG3′ (positions 1033–1011 in *dhh* exon 3); gDhh2, 5′AACTCACTGGCGGTCCGAGCCGG3′ (positions 872–893 in *dhh* exon 3); and g*neo*, 5′GGCATGCTGGGGATGCGGTG3′ (positions 3802–3822 in *pgk-neo*). PCR reactions were cycled once at 94°C for 3 min, followed by 34 rounds at 94°C for 30 s, 65°C for 20 s, 72°C for 20 s, and finally, an extension step at 72°C for 5 min. Primers gDhh1 and gDhh2 gave a 161 base pair (bp) wild-type fragment, whereas primers gDhh1 and g*neo* gave a 149 bp mutant band (data not shown).

RNA Preparation, cDNA Synthesis, and Semiquantitative RT-PCR

Total RNA was extracted from sciatic nerve freshly dissected from E13.5, E15.5, newborn, P5–P6, and adult mice or from P4–P7 rat fibroblasts with Ultraspec total RNA isolation reagent according to the manufacturer's instructions. The RNA was quantified and analyzed for integrity by agarose gel electrophoresis. Five hundred nanograms or, in the case of *hip* analysis, 5 μg of total RNA was reverse transcribed into cDNA in a 50 μl reaction containing 50 mM Tris-HCl (pH 8.3), 75 mM KCl, and 3 mM $MgCl_2$ using random hexamers as primers and Superscript II reverse transcriptase as recommended in the manufacturer's protocol. To check that the same quantity of cDNA was used in the PCR reactions, the relative amount of cDNA synthesized from each sample was assessed by PCR amplification using specific primers for 18S RNA as described previously (Owens and Boyd, 1991; Blanchard et al., 1996). One microliter of cDNA was used in 50 or 100 μl PCR reactions using the "hot start" amplification method. Reactions were cycled through one cycle at 94°C for 3 min (1 min for *hip*) followed by 33 rounds (21 for 18S and 35 for *hip*) at 94°C for 30 s; 65°C (*dhh*), 55°C (*ptc*), 50°C (*smo* and 18S), or 62°C (*hip*) for 1 min or 1 min, 30 s (*hip*); and one final extension at 72°C for 5 or 7 min. To check that the reaction was within the exponential phase of amplification, one tenth of each reaction was analyzed on a 2% gel agarose electrophoresis at 3 cycle intervals. The primer pairs were as follows (product size in parentheses): *dhh*: forward primer, 5′CATGTGGCCCGGAGTACGCC3′, reverse primer, 5′CGCTGCATCAGCGGCC AGTA3′ (346 bp); *ptc*: forward primer, 5′AACAAAAATTCAACCAAACCTTC3′, reverse primer, 5′TGTCTTCATTCCAGTTGATGTG3′ (Takabatake et al., 1997); *smo*: forward primer, 5′ATTGCCATGAGCACCTGG3′, reverse primer, 5′GCAACAGGTCCATCATGG3′ (200 bp; Akiyama et al., 1997); and *hip*: forward primer, ATCCTCCCGCGTCCTGCCCTTG, reverse primer, TCAGGCACCGTCTCCTTCTCGC (169 bp; Chuang and McMahon, 1999).

In Situ Hybridization

Digoxigenin-labeled cRNA antisense probes were generated in the presence of 0.65 mM uridine triphosphate (UTP) and 0.35 mM digoxigenin-UTP with the SP6 RNA polymerase from the SP6 promoter of a pCRII vector (Invitrogen, CA) encoding the Dhh coding sequence (Bitgood et al., 1996) cut at the single NdeI site, and with the T3 RNA polymerase of a pBSII/KS^{+} vector containing a 841 bp EcoRI fragment corresponding to the 5′ end of the mouse *ptc* cDNA (gift of Dr. M. P. Scott), linearized at the unique BamHI site. The control sense cRNA probes were synthesized from the T7 promoter of the same plasmids cut at the HindIII site.

For in situ hybridization, embryos were fixed and embedded in

polyester wax as described previously (Lee et al., 1997). Serial sections were collected on 3-amino-propyltriethoxysilane-coated slides. In situ hybridization was carried out according to a protocol adapted from Rex and Scotting (1994) as described in Blanchard et al. (1996). For teased nerve preparations, slides were fixed for 2 hr at room temperature in 4% paraformaldehyde in phosphate-buffered saline (PBS), dehydrated through an alcohol series, air dried, and stored at −70°C until required. After rehydration, teased nerve preparations were treated for 15 min in 1 mg/ml proteinase-K at 37°C and subjected to the protocol described above.

Immunohistochemistry

Sciatic nerves were dissected and immediately cryoprotected overnight in 15% sucrose in 0.1 M phosphate buffer; embedded in 7.5% gelatin, 15% sucrose in 0.1 M phosphate buffer; and frozen in liquid nitrogen–cooled isopentane. Immunohistochemistry was carried out on 10 μm cryostat sections on gelatin-coated slides. Sections were fixed for 10 min in absolute ethanol at −20°C, washed in PBS, and incubated first for 3 hr in blocking solution (0.5% blocking reagent [Boehringer], 10% sheep serum, 0.1% Triton X-100) at room temperature, and then overnight at 4°C in the presence of rabbit polyclonal anti-Cx43, anti-occludin, or anti-ZO-1 antibodies diluted 1:300, 1:200, or 1:400 in blocking solution, respectively. After washing, sections were incubated for 1 hr at room temperature with a FITC-coupled goat anti-rabbit antibody. Immunolabeling with rabbit polyclonal anti-GAP-43 was performed on in situ hybridization–treated preparations immediately after alkaline phosphatase detection. Slides were directly incubated overnight at 4°C in the presence of anti-GAP-43 antibody diluted 1:100 in PBS containing 10% calf serum and 0.1% Triton X-100. Bound antibody was detected as described above. For laminin β2, nerves were prefixed in 50% acetone, 50% ethanol for 20 min at −20°C prior to embedding and sectioning. Sections were blocked in 0.5% Triton X-100 in antibody-diluting solution (Jessen et al., 1994) for 1 hr prior to overnight incubation at 4°C in laminin β2 antibodies diluted 1:1000 in antibody-diluting solution. Bound antibody was detected with anti–guinea pig FITC (1:50) as described above. Slides were viewed and photographed either on a Zeiss Axioskop microscope or, alternatively, on a Leica TCS SP confocal microscope using TCS NT software.

Transmission and Freeze-Fracture Electron Microscopy

For transmission electron microscopy, animals were perfused intracardiacally with 1% paraformaldehyde, 1.25% glutaraldehyde in 0.1 M phosphate buffer for adults and with 2% paraformaldehyde, 2% glutaraldehyde for embryonic stages. Sciatic nerves were dissected and postfixed in the same solution for 1 hr and processed for electron microscopy. For freeze-fracture electron microscopy, nerves from normal or *dhh*$^{-/-}$ mice were fixed by perfusion or immersion fixation in 1% glutaraldehyde, 0.8% paraformaldehyde in 0.1 M Na cacodylate (pH 7.4) and glycerinated (Beamish et al., 1992). Small (1–2 mm long) pieces of glycerinated nerve were placed on squares of filter paper araldited to aluminium as described (Lawson, 1984) and frozen by plunging them into liquid nitrogen-cooled 1,1,1,2-tetrafluoroethane. Frozen samples were fractured with a Balzers BAF 400 machine at a tissue temperature of −120°C and a vacuum of $> 5 \times 10^{-6}$ torr. All samples were replicated with ~2 nm of Pt/carbon. Replicas were cleaned in 12% Na hypochlorite, rinsed in distilled water, and picked up on carbon formvar–coated grids. Images were recorded with a JEOL 1010 electron microscope operating at 100 kV.

Perineurium Permeability

A 5% bovine serum albumin (fraction V) solution in Ringer solution (pH 7.4) was mixed with Evans blue to make a 1% dye solution, EBA, which was dialyzed overnight in Ringer solution. Adult mice, both *dhh*$^{+/+}$ *and dhh*$^{-/-}$ weighing 22–35 g, were used. Under anesthesia, 50 μl of EBA was injected through the fascia over the sciatic nerve without freeing the nerve from the surrounding tissue. One hour after injection, animals were perfused intracardially with 4% paraformaldehyde in PBS. Sciatic nerves were dissected, cryoprotected, embedded in gelatin, and frozen in liquid nitrogen–cooled isopentane (see immunochemistry). Cryostat sections 10 μm thick were mounted in 50% glycerol in water and viewed immediately under a fluorescence microscope. In another set of experiments using the same surgical procedure, animals were injected with a suspension of 10^8 heat-killed *E. coli* in 50 ml of PBS or with PBS only. Animals were sacrificed 24 hr after operation. Sciatic nerves were dissected, fixed overnight in 4% paraformaldehyde in PBS, and embedded in polyester wax. Sections, 10 μm thick, were stained with hematoxylin and eosin. Alternatively, gelatin-mounted frozen sections were acetone fixed and treated with biotinylated antibody Ly-6G (Gr-1). In peripheral tissues, it specifically recognizes neutrophils from normal and *dhh*$^{-/-}$ mice (Lagasse and Weissman, 1996). It was used at a dilution of 1:100 overnight (Pharmingen). Streptavidin-FITC, diluted 1:100, was used as a second layer.

Cell Culture Experiments

P4–P7 nerve fibroblasts were purified by immunopanning using antibodies to Thy-1 and were a gift from Drs. D. Parkinson and E. Calle (Lee et al., 1997). Fibroblasts were grown in 9 cm diameter tissue culture dishes in Dulbecco's modified Eagle's medium and 10% fetal calf serum at 37° in 5% CO_2. In four separate experiments for *ptc* and *smo* and two experiments for *hip*, recombinant human Dhh, a gift from Biogen, was added at doses from 5 to 20 nM for periods of 2–24 hr prior to RNA extraction and semiquantitative RT-PCR.

Electrophysiology

Two to four adult *dhh*$^{-/-}$ mice were compared with two to four *dhh*$^{+/+}$ littermates of the same age; weights were between 30 and 35 g. Animals were anesthetized with urethane (1.5 g/kg, intraperitoneally). Rectal temperature and nerve temperature were monitored with thermocouples. The saphenous nerve was isolated in the medial thigh, and compound action potentials were recorded directly under mineral oil as described previously in the rat (Baranowski et al., 1986). Nerve fibers were stimulated with 0.05 ms (A fibers) or 0.5 ms (C fibers) duration constant current pulses. Fine platinum wire electrodes were used for both stimulation and recording, and the conduction velocity was calculated from the change in latency and at different distances (3–12 mm) between stimulating and recording electrodes. The pool temperatures were 31°C–34°C. The sciatic nerve was exposed in the posterior thigh and stimulated with 0.05 ms pulses via fine platinum wire electrodes, at different positions. The muscle action potential was recorded from the calf muscles (gastrocnemius/soleus) with a concentric needle electrode, and the conduction velocity was calculated from the change in latency with stimulation location along the nerve.

Acknowledgments

This work was supported by the Wellcome Trust and the EC. D. L. was the recipient of an award from the British United Provident Association. E. P. was the recipient of a Training and Mobility of Researchers fellowship from the EC. We thank Professor S. M. Hall for drawing our attention to the minifascicles and Professor P. K. Thomas, Dr. R. King, and Dr. M. B. Bunge for extensive discussion and advice. We thank Dr. J. Roes for the gift of fixed *E. coli* and *Staphylococcus aureus*, the Ly6-G antibody, and expert advice. We thank Dr. R. Curtis for the GAP-43 antibody, Dr. R. Dermietzel for the Cx43 antibody, Dr. J. Sanes for the laminin β2 antibody, Dr. L. Morgan for ZO-1 antibodies, Dr. M. P. Scott for the *ptc* probe, and Biogen for the recombinant human Dhh. We thank Dr. D. Parkinson and Dr. E. Calle for fibroblasts, Mr. B. Harris for expert advice and help with electron microscopy, Mrs. G. Brady for histology, Ms. K. Langner for technical assistance, Mr. D. Clements for help with image analysis, and Mrs. D. Bartram for editing the manuscript.

Received December 17, 1998; revised June 24, 1999.

References

Ahmed, A.M., and Weller, R.O. (1979). The blood–nerve barrier and reconstitution of the perineurium following nerve grafting. Neuropath. Appl. Neurobiol. *5*, 469–483.

Akiyama, H., Shigeno, C., Hiraki, Y., Shukunami, C., Kohno, H., Akagi,

M., Konishi, J., and Nakamura, T. (1997). Cloning of a mouse smoothened cDNA and expression patterns of hedgehog signalling molecules during chondrogenesis and cartilage differentiation in clonal mouse EC cells, ATDC5. Biochem. Biophys. Res. Commun. *235*, 142–147.

Baranowski, R., Lynn, B., and Pini, A. (1986). The effects of locally applied capsaicin on conduction in cutaneous nerves in four mammalian species. Br. J. Pharmacol. *89*, 267–276.

Beamish, N.G., Stolinski, C., Thomas, P.K., King, R.H., and Rud, A. (1992). A freeze-fracture study of the perineurium in galactose neuropathy: morphological changes associated with endoneurial oedema. J. Neurocytol. *21*, 67–78.

Bitgood, M.J., and McMahon, A.P. (1995). Hedgehog and Bmp genes are coexpressed at many diverse sites of cell–cell interaction in the mouse embryo. Dev. Biol. *172*, 126–138.

Bitgood, M.J., Shen, L., and McMahon, A.P. (1996). Sertoli cell signaling by Desert hedgehog regulates the male germline. Curr. Biol. *6*, 298–304.

Blanchard, A.D., Sinanan, A., Parmantier, E., Zwart, R., Broos, L., Meijer, D., Meier, C., Jessen, K.R., and Mirsky, R. (1996). Oct-6 (SCIP/Tst-1) is expressed in Schwann cell precursors, embryonic Schwann cells, and postnatal myelinating Schwann cells: comparison with Oct-1, Krox-20, and Pax-3. J. Neurosci. Res. *46*, 630–640.

Bradley, J.L., Abernethy, D.A., King, R.H.M., Muddle, J.R., and Thomas, P.K. (1998). Neural architecture in transected rabbit sciatic nerve after prolonged non-reinnervation. J. Anat. *192*, 529–538.

Bunge, M.B., Wood, P.M., Tynan, L.B., Bates, M.L., and Sanes, J.R. (1989). Perineurium originates from fibroblasts: demonstration in vitro with a retroviral marker. Science *243*, 229–231.

Chandross, K.J., Kessler, J.A., Cohen, R.I., Simburger, E., Spray, D.C., Bieri, P., and Dermietzel, R. (1996). Altered connexin expression after peripheral nerve injury. Mol. Cell. Neurosci. *7*, 501–518.

Chen, Y., and Struhl, G. (1996). Dual roles for patched in sequestering and transducing hedgehog. Cell *87*, 553–563.

Chuang, P.-T., and McMahon, A.P. (1999). Vertebrate Hedgehog signalling modulated by induction of a Hedgehog-binding protein. Nature *397*, 617–621.

Curtis, R., Stewart, H.J.S., Hall, S.M., Wilkin, G.P., Mirsky, R., and Jessen, K.R. (1992). GAP-43 is expressed by non-myelin-forming Schwann cells of the peripheral nervous system. J. Cell Biol. *117*, 225–238.

Dong, Z., Brennan, A., Liu, N., Yarden, Y., Lefkowitz, G., Mirsky, R., and Jessen, K.R. (1995). NDF is a neuron-glia signal and regulates survival, proliferation, and maturation of rat Schwann cell precursors. Neuron *15*, 585–596.

Dong, Z., Sinanan, A., Parkinson, D., Parmantier, E., Mirsky, R., and Jessen, K.R. (1999). Schwann cell development in embryonic mouse nerves. J. Neurosci. Res. *56*, 334–348.

Elias, P.M., and Friend, D.S. (1976). Vitamin-A-induced mucous metaplasia. An in vitro system for modulating tight and gap junction differentiation. J. Cell Biol. *68*, 173–188.

Fujimoto, K., Nagafuchi, A., Tsukita, S., Kuraoka, A., Ohokuma, A., and Shibata, Y. (1997). Dynamics of connexins, E-cadherin and alpha-catenin on cell membranes during gap junction formation. J. Cell Sci. *110*, 311–322.

Furuse, M., Hirase, T., Itoh, M., Nagafuchi, A., Yonemura, S., Tsukita, S., and Tsukita, S. (1993). Occludin: a novel integral membrane protein localizing at tight junctions. J. Cell Biol. *123*, 1777–1788.

Furuse, M., Fujita, K., Hiiragi, T., Fujimoto, K., and Tsukita, S. (1998a). Claudin-1 and -2: novel integral membrane proteins localizing at tight junctions. J. Cell Biol. *141*, 1539–1550.

Furuse, M., Sasaki, H., Fujimoto, K., and Tsukita, S. (1998b). A single gene product, claudin-1 or -2, reconstitutes tight junction strands and recruits occludin in fibroblasts. J. Cell Biol. *143*, 391–401.

Gold, R., Archelos, J.J., and Hartung, H.P. (1999). Mechanisms of immune regulation in the peripheral nervous system. Brain Pathol. *9*, 343–360.

Goodrich, L.V., Johnson, R.L., Milenkovic, L., McMahon, J.A., and Scott, M.P. (1996). Conservation of the hedgehog/patched signaling pathway from flies to mice: induction of a mouse *patched* gene by hedgehog. Genes Dev. *10*, 301–312.

Greening, J., and Lynn, B. (1998). Minor peripheral nerve injuries: an underestimated source of Pain? Manual Ther. *3*, 187–194.

Hall, S.M. (1989). Regeneration in the peripheral nervous system. Neuropath. Appl. Neurobiol. *15*, 513–529.

Hammerschmidt, M., Brook, A., and McMahon, A.P. (1997). The world according to *hedgehog*. Trends Genet. *13*, 14–21.

Ingham, P.W. (1998). Transducing hedgehog: the story so far. EMBO J. *17*, 3505–3511.

Jessen, K.R., and Mirsky, R. (1999). Schwann cells and their precursors emerge as important regulators of nerve development. Trends Neurosci., in press.

Jessen, K.R., Brennan, A., Morgan, L., Mirsky, R., Kent, A., Hashimoto, Y., and Gavrilovic, J. (1994). The Schwann cell precursor and its fate: a study of cell death and differentiation during gliogenesis in rat embryonic nerves. Neuron *12*, 509–527.

Kojima, T., Yamamoto, M., Tobioka, H., Miziguchi, T., Mitaka, T., and Mochizuki, Y. (1996). Changes in cellular distribution of connexins 32 and 23 during formation of gap junctions in primary cultures of rat hepatocytes. Exp. Cell Res. *223*, 314–326.

Kristensson, K., and Olsson, Y. (1971). The perineurium as a diffusion barrier to protein tracers. Differences between mature and immature animals. Acta Neuropathol. *17*, 127–138.

Lagasse, E., and Weissman, I.L. (1996). Flow cytometric identification of murine neutrophils and lymphocytes. J. Immunol. Meth. *197*, 139–150.

Lawson, D. (1984). Distribution of epinemin in colloidal gold-labelled, quick-frozen, deep-etched cytoskeletons. J. Cell Biol. *99*, 1451–1460.

Lee, M.-J., Brennan, A., Blanchard, A., Zoidl, G., Dong, Z., Tabernero, A., Zoidl, C., Dent, M.A.R., Jessen, K.R., and Mirsky, R. (1997). P_0 is constitutively expressed in the rat neural crest and embryonic nerves and is negatively and positively regulated by axons to generate non-myelin-forming and myelin-forming Schwann cells, respectively. Mol. Cell. Neurosci. *8*, 336–350.

McCarthy, K.M., Skare, I.B., Stankewich, M.C., Furuse, M., Tsukita, S., Rogers, R.A., Lynch, R.D., and Schneeburger, E.E. (1996). Occludin is a functional component of the tight junction. J. Cell Sci. *109*, 2287–2298.

Olsson, Y. (1990). Microenvironment of the peripheral nervous system under normal and pathological conditions. Crit. Rev. Neurobiol. *5*, 265–311.

Owens, G.C., and Boyd, C.J. (1991). Expressing antisense P0 RNA in Schwann cells perturbs myelination. Development *112*, 639–649.

Porter, B.E., and Sanes, J.R. (1995). Gated migration: neurons migrate on but not onto substrates containing S-laminin. Dev. Biol. *167*, 609–616.

Rex, M., and Scotting, P.J. (1994). Simultaneous detection of RNA and protein in tissue sections by nonradioactive in situ hybridisation followed by immunohistochemistry. Biochemica *3*, 24–28.

Rosenbaum, T., Boissy, Y.L., Kombrinck, K., Brannan, C.I., Jenkins, N.A., Copeland, N.G., and Ratner, N. (1995). Neurofibromin-deficient fibroblasts fail to form perineurium in vitro. Development *121*, 3583–3592.

Saitou, M., Fujimoto, K., Doi, Y., Itoh, M., Fujimoto, T., Furuse, M., Takano, H., Noda, T., and Tsukita, S. (1998). Occludin-deficient embryonic stem cells can differentiate into polarized epithelial cells bearing tight junctions. J. Cell Biol. *141*, 397–408.

Sanes, J.R., Engvall, E., Butkowski, R., and Hunter, D.D. (1990). Molecular heterogeneity of basal laminae: isoforms of laminin and collagen IV at the neuromuscular junction and elsewhere. J. Cell Biol. *111*, 1685–1699.

Schiavinato, A., Morandin, A.R., Guidolin, D., Lini, E., Nunzi, M.G., and Fiori, M.G. (1991). Perineurium of sciatic nerve in normal and diabetic rodents: freeze-fracture study of intercellular junctional complexes. J. Neurocytol. *20*, 459–470.

Simon, A.M., and Goodenough, D.A. (1998). Diverse functions of vertebrate gap junctions. Trends Cell Biol. *8*, 477–482.

Stevenson, B.R., Siliciano, J.D., Mooseker, M.S., and Goodenough, D.A. (1986). Identification of ZO-1: a high molecular weight polypeptide associated with the tight junction (zonula occludens) in a variety of epithelia. J. Cell Biol. *103*, 755–766.

Stone, D.M., Hynes, M., Armanini, M., Swanson, T.A., Gu, Q., Johnson, R.L., Scott, M.P., Pennica, D., Goddard, A., Phillips, H. et al. (1996). The tumour-suppressor gene patched encodes a candidate receptor for Sonic hedgehog. Nature *14*, 129–134.

Tabin, C.J., and McMahon, A.J. (1997). Recent advances in Hedgehog signalling. Trends Cell Biol. *7*, 442–446.

Takabatake, T., Ogawa, M., Takahashi, T.C., Mizuno, M., Okamoto, M., and Takeshima, K. (1997). Hedgehog and patched gene expression in adult ocular tissues. FEBS Lett. *410*, 485–489.

Thomas, P.K., and Bhagat, S. (1978). The effect of extraction of intrafascicular contents of peripheral nerve trunks on perifascicular structure. Acta Neuropathol. (Berl) *43*, 135–140.

Thomas, P.K., and Jones, D.G. (1965). The cellular response to nerve injury. J. Anat. *101*, 45–55.

Thomas, P.K., and Olsson, Y. (1984). Microscopic anatomy and function of the connective tissue components of peripheral nerve. In Peripheral Neuropathy, Volume 1, P.J. Dyck et al., eds. (Philadelphia: Saunders), pp. 97–120.

Thomas, P.K., Landon, D.N., and King, R.H.M. (1990). Diseases of the peripheral nerves. In Greenfield's Neuropathology, Sixth Edition, D.I. Graham and P.L. Lantos, eds. (London: Arnold), pp. 409–414.

Vanderburg, C.M., and Hay, E.M. (1996). E-cadherin transforms embryonic corneal fibroblasts to stratified epithelium with desmosomes. Acta Anat. (Basel) *157*, 87–104.

Vortkamp, A., Lee, K., Lanske, B., Segre, G.V., Kronenberg, H.M., and Tabin, C.J. (1996). Regulation of cartilage differentiation by Indian Hedgehog and PTH-related protein. Science *273*, 613–622.

Wong, V., and Gumbiner, B.M. (1997). A synthetic peptide corresponding to the extracellular domain of occludin perturbs the tight junction permeability barrier. J. Cell Biol. *136*, 399–409.